



Extracerebral Tissue Damage in the Intraluminal Filament Mouse Model of Middle Cerebral Artery Occlusion

Markus Vaas¹, Ruiqing Ni¹, Markus Rudin^{1,2}, Anja Kipar³ and Jan Klohs^{1*}

¹Institute for Biomedical Engineering, University of Zurich, ETH, Zurich, Switzerland, ²Institute of Pharmacology and Toxicology, University of Zurich, Zurich, Switzerland, ³Institute of Veterinary Pathology, University of Zurich, Zurich, Switzerland

Middle cerebral artery occlusion is the most common model of focal cerebral ischemia in the mouse. In the surgical procedure, the external carotid artery (ECA) is ligated; however, its effect on the tissue supplied by the vessel has not been described so far. C57BL/6 mice underwent 1 h of transient MCAO (tMCAO) or sham surgery. Multi-spectral optoacoustic tomography was employed at 30 min after surgery to assess oxygenation in the temporal muscles. Microstructural changes were assessed with magnetic resonance imaging and histological examination at 24 h and 48 h after surgery. Ligation of the ECA resulted in decreased oxygenation of the left temporal muscle in most sham-operated and tMCAO animals. Susceptible mice of both groups exhibited increased T_2 relaxation times in the affected muscle with histological evidence of myofibre degeneration, interstitial edema, and neutrophil influx. Ligatures had induced an extensive neutrophil-dominated inflammatory response. ECA ligation leads to distinct hypoxic degenerative changes in the tissue of the ECA territory and to ligation-induced inflammatory processes. An impact on outcome needs to be considered in this stroke model.

Keywords: middle cerebral artery occlusion, mouse, ischemia, external carotid artery, muscle degeneration

OPEN ACCESS

Edited by:

Thanh G. Phan,
Monash Health, Australia

Reviewed by:

Christoph Harms,
Charité Universitätsmedizin Berlin,
Germany

Muzamil Ahmad,
Indian Institute of Integrative
Medicine, India

*Correspondence:

Jan Klohs
klohs@biomed.ee.ethz.ch

Specialty section:

This article was submitted to Stroke,
a section of the journal
Frontiers in Neurology

Received: 16 January 2017

Accepted: 24 February 2017

Published: 13 March 2017

Citation:

Vaas M, Ni R, Rudin M, Kipar A and
Klohs J (2017) Extracerebral Tissue
Damage in the Intraluminal Filament
Mouse Model of Middle Cerebral
Artery Occlusion.
Front. Neurol. 8:85.
doi: 10.3389/fneur.2017.00085

INTRODUCTION

Rodent models of cerebral ischemia are employed for studying pathophysiological mechanisms and for preclinical drug testing (1). Among them, proximal middle cerebral artery occlusion (MCAO) with an intraluminal suture is a well-characterized and widely accepted model of focal cerebral ischemia. In MCAO, the common carotid artery (CCA) is surgically exposed, and a suture is inserted into the CCA, advanced into the internal carotid artery (ICA) until the branch of the middle cerebral artery (MCA), to transiently or permanently interrupt blood flow to the MCA territory. The procedure requires ligation of the external carotid artery (ECA) and thereby also restricts perfusion of the extracerebral ECA territory. In rats, hyperintensities in T_2 -weighted magnetic resonance images (MRI) and histological evidence of myofibre degeneration and regeneration were reported on day 5 after MCAO (2). ECA ligation was associated with delayed body weight recovery and impaired motor recovery compared to procedures where the ECA was not ligated (2, 3).

Despite the wide usage of the mouse MCAO model, the effects of ECA ligation have not so far been investigated in this species. In a recent study, we observed neutrophil influx into the ipsilateral temporal muscles in mice after 1 h of transient MCAO (tMCAO) or sham surgery (4). This has

prompted us to further investigate the effects of ECA ligation on tributary tissues in the mouse MCAO model.

MATERIALS AND METHODS

Animals

All procedures conformed to the national guidelines of the Swiss Federal act on animal protection and were approved by the Cantonal Veterinary Office Zurich (Permit Number: 18-2014). All procedures fulfill the ARRIVE guidelines on reporting animal experiments. Male C57BL/6J mice (Janvier, France), weighing 20–25 g, of 8–10 weeks of age were used. Animals were housed in a temperature controlled room in individually ventilated cages, under a 12-h dark/light cycle. Paper tissue was given as environmental enrichment. Access to pelleted food (3437PXL15, CARGILL) and water were provided *ad libitum*.

Study Design

Using G*Power 3.1 software (Heinrich-Heine-University, Düsseldorf, Germany; <http://www.gpower.hhu.de/>), a group size of $n = 4$ was determined *a priori* for the primary end point T_2 relaxation time, with an effect size $d = 2.0$, $\alpha = 0.05$ and $\beta = 0.2$. Consequently, group sizes of $n > 4$ were used.

In total, 45 mice were randomly allocated to tMCAO or sham surgery (Table 1). For randomization, the web tool www.randomizer.org was used. Animals received randomized numbers and were randomly allocated to their cages and groups. Surgeries were performed in a random order, while the experimenter was blinded to the group until the insertion of the filament during the surgery.

The number of animals that were used for each study and number of animals that were excluded from final analysis are depicted in Table 1. One group of animals underwent assessment of muscle tissue oxygenation with multispectral optoacoustic tomography (MSOT) at 30 min after induction of tMCAO or sham surgery. A second group of animals underwent MRI examination at 24 and 48 h after reperfusion. Due to technical reasons, fewer animals were measured at the 24 h than at the 48 h time point. A third group of animals were transcatheterially perfused and prepared for histological analysis at 24 h after

reperfusion. The unaffected contralateral side was considered to reflect the baseline values. We performed evaluation of all read-out parameters, while blinded to the experimental groups.

The following criteria were used to exclude animals from the end-point analysis: (i) subarachnoidal or intracerebral hemorrhage, (ii) no reflow after filament withdrawal, (iii) Bederson score = 0 (only in MCAO groups), and (iv) dead before experimental endpoint.

Transient MCAO

Surgical procedures were performed as described previously (4, 5). In brief, anesthesia was initiated by using 3% isoflurane (Abbott, Cham, Switzerland) in a mixture of O₂ (200 ml/min) and air (800 ml/min) and maintained with 1.5–2% isoflurane. Before the surgical procedure, a local analgesic (Lidocaine, 0.5%, 7 mg/kg) was administered subcutaneously. Temperature was controlled during the surgery and kept constant at $36.5 \pm 0.5^\circ\text{C}$ with a feedback-heating controlled pad system. For tMCAO, a midline neck incision was made and the left CCA was ligated proximal of the bifurcation of the ICA and ECA. Subsequently, the left ECA was isolated and ligated and a suture was placed around the ICA. A small incision was made in the CCA and an 11-mm long silicone monofilament (701956PK5Re; Doccol Corporation, USA) was introduced and advanced until it occluded the MCA and left in place for 60 min. A suture around the ICA secured the filament in position. Animals were transferred to a heated recovery box and allowed to wake up. Animals were reanaesthetized, the filament was withdrawn and the ICA was ligated. Sham operation involved surgical procedures, without occlusion of the MCA. After surgery, buprenorphine was administered as s.c. injection (Temgesic, 0.1 mg/kg body weight) and animals were placed in a heated recovery box for 2 h. Buprenorphine was then given twice s.c. every 6–8 h on the day of surgery and thereafter supplied *via* drinking water (1 mg/kg) for 36 h. Animals received softened chow in a petri dish placed on the floor of their cages to encourage eating.

Multi-Spectral Optoacoustic Tomography

For MSOT, mice were anesthetized with 1.5–2% isoflurane in an oxygen/air mixture (1:4). The fur overlying the head was first trimmed with an electrical shaver and then hair was removed by using a depilation cream (Nair). Mice were placed in a mouse holder in supine position. Isoflurane anesthesia (1.5%) in an oxygen/air mixture was supplied *via* a nose cone. Ultrasound gel (Diagramma, Switzerland) was applied to the mouse head for ultrasonic coupling and the animals were wrapped in a polyethylene membrane. The mouse holder was placed in an acquisition chamber filled with water for acoustic coupling. Water was kept 34°C to maintain body temperature while imaging.

The MSOT inVision 128 small animal imaging system was previously described (6). Briefly, a tunable optical parametric oscillator pumped by an Nd:YAG laser provides excitation pulses with a duration of 9 ns at wavelengths from 680 to 980 nm at a repetition rate of 10 Hz with a wavelength tuning speed of

TABLE 1 | Overview summarizing the number of animals for each study, with number of animals that were excluded from final analysis.

		Total animals: $n = 45$		
		Total	Excluded	Exclusion criteria
MSOT	Sham	10	3	Non-responder
	tMCAO	9	2	Non-responder
MRI	Sham 24 h	11	6	$n = 1$ non-responder; $n = 5$ technical reasons
	Sham 48 h	11	1	Non-responder
	tMCAO 24 h	7	2	$n = 1$ non-responder; $n = 1$ technical reasons
	tMCAO 48 h	7	1	Non-responder
Histology	Sham	4	0	
	tMCAO	4	0	

10 ms and a peak pulse energy of 100 mJ at 730 nm. Ten arms of a fiber bundle provide even illumination of a ring-shaped light strip of approximately 8 mm width. For ultrasound detection, 128 cylindrically focused ultrasound transducers with a center frequency of 5 MHz (60% bandwidth), organized in a concave array of 270° angular coverage and a radius of curvature of 4 cm, were used. Imaging was performed at six wavelengths (715, 730, 760, 800, 850 to 900 nm), at 35–40 consecutive slices with a step size of 0.3 mm, and at 10 averages.

Magnetic Resonance Imaging

Data was acquired on a 4.7 T Bruker PharmaScan 47/16 (Bruker BioSpin GmbH), equipped with a volume resonator operating in quadrature mode for excitation and a four-element phased array surface coil for signal reception. During MRI acquisition, mice were kept under isoflurane anesthesia 1.5% in a 4:1 air/oxygen mixture. Body temperature was monitored with a rectal temperature probe (MLT415, ADInstruments) and kept at $36 \pm 0.5^\circ\text{C}$ using a warm water circuit integrated into the animal support (Bruker BioSpin GmbH). First, one sagittal 2D slice was acquired with a true fast imaging with steady state precession (TrueFISP) sequence to reproducibly position the image slices for the T_2 map between animals and different days of assessment. The TrueFISP sequence was applied with the following parameters: echo time (TE) = 3 ms, repetition time (TR) = 6 ms, 100 averages, slice thickness = 1 mm, field of view (FOV) = $2.56 \text{ cm} \times 1.28 \text{ cm}$, and matrix size = $256 \text{ mm} \times 128 \text{ mm}$, giving an in-plane resolution (IR) = $100 \mu\text{m} \times 100 \mu\text{m}$. For time-of-flight MR angiography a 3D FLASH sequence with the parameters TE = 3 ms, TR = 12 ms, $\alpha = 20^\circ$, 3 averages, FOV = $20 \text{ mm} \times 20 \text{ mm} \times 20 \text{ mm}$, and a matrix size = $256 \text{ mm} \times 256 \text{ mm} \times 256 \text{ mm}$, resulting in an IR = $78 \mu\text{m}^3$ were acquired. To assess the T_2 relaxation time of muscle tissue, a 2D Carr-Purcell-Meiboom-Gill multi-slice-multi-echo sequence was performed with 14 echoes, TE1 = 12 ms, an inter-echo time = 12 ms, TR = 2783 ms, averages = 4, FOV = $20 \text{ mm} \times 20 \text{ mm}$, and matrix size = $100 \text{ mm} \times 100 \text{ mm}$, giving an IR = $200 \mu\text{m} \times 200 \mu\text{m}$.

MSOT Image Reconstruction and Spectral Unmixing

Images were reconstructed using a backprojection algorithm with a non-negativity constraint imposed during inversion (7). Linear unmixing was applied to resolve signals from deoxygenated and oxygenated hemoglobin (8). For each pixel in the image, the method fits the total measured optoacoustic spectrum to the known absorption spectra of oxy- and deoxy-hemoglobin. On axial cross sections of the mouse head regions of interest were drawn over the left ischemic (ipsi) and right (contra) temporal muscle regions (Figure 1). Oxygen saturation of each region was calculated according to the following formula:

$$sO_2 = \text{HbO}_2 / \text{Hb} + \text{HbO}_2 \quad (1)$$

The ratios of sO_2 values between the ipsi- and contralateral sides were calculated.

MRI Data Processing and Analysis

T_2 maps were computed using Paravision software (Bruker) by mono-exponential fitting of the spin-echo magnitude signal decay, S ,

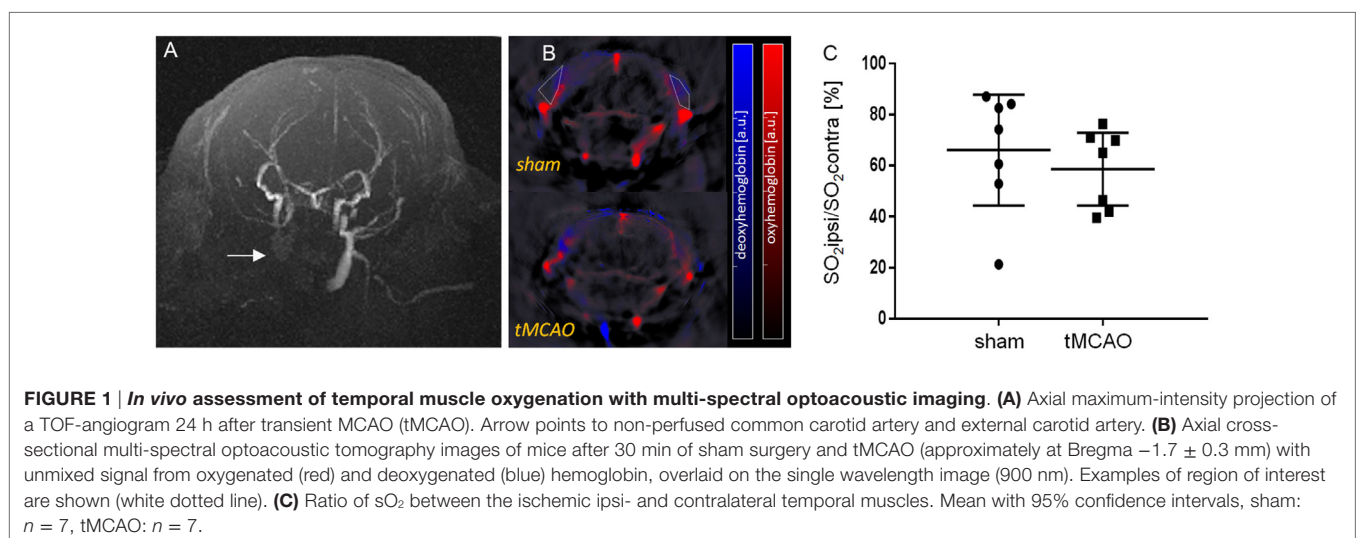
$$S = S_0 \exp\left(-\frac{TE}{T_2}\right) \quad (2)$$

where both S_0 , the signal at TE = 0, and T_2 , the irreversible relaxation time, are fitted.

Regions-of-interest were drawn on T_2 maps around the temporal muscle identified on the ipsi- and contralateral side of the mouse head on four consecutive images.

Histology

Animals were put under deep anesthesia by intraperitoneal injection of ketamine/xylazine/acepromazine maleate (100/20/3 mg/kg body weight) and transcardially perfused with 20 ml PBS, followed by 1% paraformaldehyde [(PFA); pH 7.4] in PBS. Whole heads were removed, skinned, and



fixed in 4% PFA for approximately 48 h. After decalcification in EDTA–citric acid buffer (pH 7.5, BioCYC GmbH & Co KG, Potsdam, Germany), coronal sections were applied to prepare two slices of the brain, which were then routinely paraffin wax embedded. Consecutive sections (3–5 μm) were prepared and stained with hematoxylin eosin.

Statistical Analysis

Comparisons between groups were made by a Mann–Whitney rank sum test and Student's *t*-test (SigmaPlot 12.5). A *p*-value < 0.05 was considered significant.

RESULTS

All raw data are made available in a data repository (9).

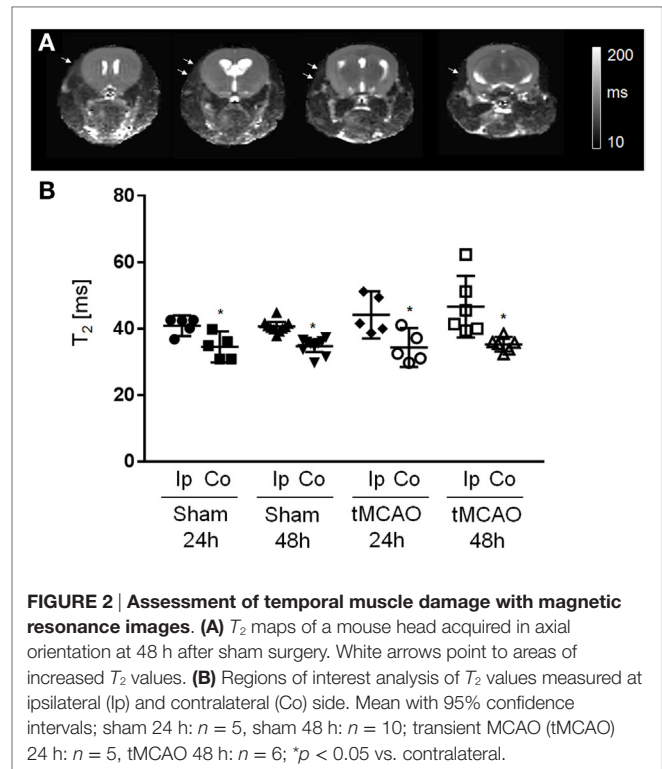
Arrest of Blood Flow in ECA Territory Caused Reduced Tissue Oxygenation in Temporal Muscle

Ligation of the CCA and ECA led to an arrest of blood flow in the corresponding vessel (Figure 1A) and reduced tissue oxygenation (Figures 1B,C). Quantification of tissue oxygenation in the temporal muscle showed reduced sO_2 values in 7 out of 10 sham and 7 out of 9 tMCAO animals compared to the contralateral side (Figure 1C, mean \pm confidence intervals, sO_2 sham $66 \pm 22\%$ and tMCAO $59 \pm 14\%$ vs. 100%, $p < 0.05$, excluding non-responders).

Tissue Damage in the ECA Territory

We inspected parametric T_2 maps of tMCAO and sham-operated animals at 24 and 48 h after surgery (Figure 2A). At the final time point, 10 out of 11 sham and 6 out of 7 tMCAO animals showed increased T_2 relaxation times in the left temporal muscle. Statistical analysis (excluding mice with no differences in T_2 values) showed significantly higher T_2 values between the ipsilateral and contralateral temporal muscle, both at 24 and 48 h after surgery (Figure 2B, mean \pm confidence intervals, T_2 sham 40.9 ± 3.1 ms vs. 34.5 ± 4.7 ms and 40.7 ± 1.3 ms vs. 34.7 ± 1.7 ms; tMCAO 44.2 ± 7.1 ms vs. 34.3 ± 5.8 ms and 46.6 ± 9.3 ms vs. 35.3 ± 1.2 ms, at 24 h and 48 h after surgery, respectively, $p < 0.05$), with no differences between sham surgery and tMCAO.

The histological examination of cross sections prepared from the whole head of tMCAO mice at 24 h after reperfusion (Figures 3A–D) confirmed the presence of degenerated myofibers in the ipsilateral temporal muscle, though of a variable degree (Figure 3B). This was generally associated with evidence of neutrophil recruitment into the muscle and mild interstitial edema. Rare individual degenerate fibers were also seen in the ipsilateral temporal muscle of sham-operated mice (data not shown). The contralateral muscle was unaltered. However, myofiber degeneration was also observed in other muscles of the ECA territory, in particular the masseter muscle bulks, where it was generally more intense than in the temporal muscle, and associated with neutrophil influx (Figure 3C). In addition, intense focal neutrophil-dominated inflammatory infiltration



with surrounding edema was present at the site of ECA ligation (Figure 3D). In some cases, this extended to the cervical ganglion and was even associated with neuronal necrosis and neutrophil infiltration of the ganglion.

DISCUSSION

We demonstrated that ECA ligation required for tMCAO/sham procedure results in acute reduction of tissue oxygenation and in subsequent tissue damage. Generally, a high variability in read-outs was observed between animals. This might be likely due to differences in vascular architecture of individual animals (10). Animals with marked collateral blood supply to the ECA territory are probably less susceptible to ischemia after ECA ligation, whereas littermates with poorer collateralization might tend to develop ischemic damage after the experimental procedure. Given the differences in vascular architecture between different mouse strains (10), the effect of ECA ligation may differ in strains other than C57BL/6.

Skeletal muscle is more tolerant to ischemia than the brain and requires several hours of ischemia before damage manifests (11). In the MCAO model, the ECA ligation is not reversed and we have shown that this leads to increased T_2 values. Histological examination revealed myofiber degeneration, edema, and neutrophil influx in areas of increased T_2 . In addition to the ischemic muscle damage, ECA ligation induced local inflammatory processes in the vessel wall and surrounding tissues, where the inflammatory processes can even involve the cervical ganglion.

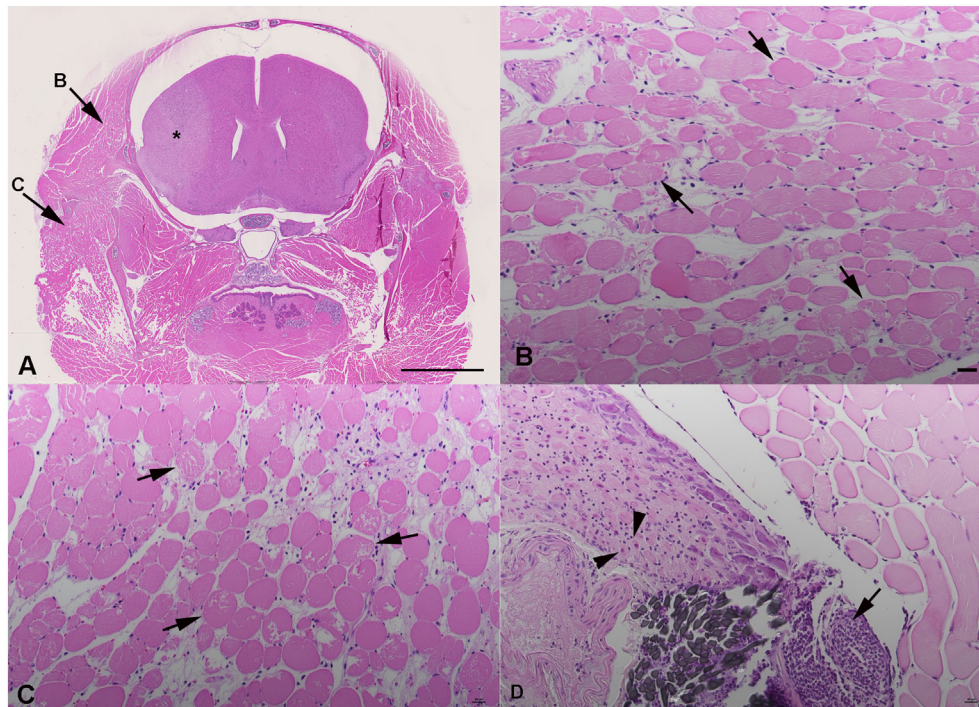


FIGURE 3 | Histological findings in transient MCAO mouse, 24 h after reperfusion. Hematoxylin eosin stains. Coronal section of the head at Bregma 1.1 mm (A–C). (A) Overview, indicating the cerebral lesion (*), the affected temporal muscle (B) and masseter muscle (C). Scale bar = 2.5 mm. (B) Ipsilateral temporal muscle with myofibers undergoing degeneration (arrows) and mild interstitial edema. (C) Ipsilateral masseter muscle with myofibre degeneration (arrows). There is moderate interstitial edema with several neutrophils in interstitial capillaries. (D) Ligature (gray suture material) with intense focal neutrophil infiltration (arrow) extending into the adjacent cervical ganglion. The ganglion exhibits neuronal necrosis (arrowheads) and a mild neutrophil infiltration. (B–D) Scale bar = 20 μ m.

In the current study, we have not investigated functional consequences of ECA ligation. However, it was previously reported that tMCAO leads to weight loss, ischemia-induced muscle wasting, and reduced food intake, which is correlated with lesion volume (12). Based on the results of the present study, one could speculate that the tMCAO and even the surgery alone can be responsible for some of the decreased food intake, both due to muscle degeneration in the ECA territory and due to surgery-associated local inflammatory processes that are associated with pain and/or affect the sympathetic nervous system. Extensive muscle damage can lead to impaired function of muscles involved in mastication and swallowing and myalgia. Studies have previously described the impairment of motor function in the intraluminal tMCAO model in rats (2, 3). Moreover, ischemia of the skeletal muscles leads to a systemic inflammatory response (13), which might affect the dynamics and distribution of immune cells in the tMCAO model. Indeed, we reported an increase in the proportion of circulating neutrophils in the blood of sham-operated animals similar to tMCAO mice (4). Also, muscle ischemia leads to factor XII-driven contact-induced activation of the coagulation system and can induce coagulopathy (14). Though the execution and duration of the surgery might affect these

described parameters, also the type of anesthesia and analgesia, the effects of ECA tissue damage on the read-outs need to be considered (15, 16). A possible solution to prevent muscle damage in the ECA territory is to reperfuse the CCA and the ECA also after retraction of the filament. This would require closing the incision in the CCA and might thus be technically very challenging.

In summary, ECA ligation leads to variable tissue damage. Its confounding impact on study parameters in experimental stroke studies needs to be further investigated.

AUTHOR CONTRIBUTIONS

MV, AK, and JK conceived and designed the experiments. MV, RN, and AK performed the experiments. MV, RN, AK, and JK analyzed the data. MV, RN, AK, MR, and JK interpreted results. JK wrote the paper. All coauthors made critical revisions to the manuscript.

FUNDING

The work was funded by the Swiss National Science Foundation (Grant PZ00P3_136822) and the Hartmann-Müller Foundation.

REFERENCES

1. Carmichael ST. Rodent models of focal stroke: size, mechanism, and purpose. *NeuroRx* (2005) 2:396–409. doi:10.1602/neurorx.2.3.396
2. Dittmar M, Spruss T, Schuierer G, Horn M. External carotid artery territory ischemia impairs outcome in the endovascular filament model of middle cerebral artery occlusion in rats. *Stroke* (2003) 34:2252–7. doi:10.1161/01.STR.0000083625.54851.9A
3. Trueman RC, Harrison DJ, Dwyer DM, Dunnett SB, Hoehn M, Farr TD. A critical re-examination of the intraluminal filament MCAO Model: impact of external carotid artery transection. *Transl Stroke Res* (2011) 2:651–61. doi:10.1007/s12975-011-0102-4
4. Vaas M, Enzmann G, Perinat T, Siler U, Reichenbach R, Licha K, et al. Non-invasive near-infrared fluorescence imaging of the neutrophil response in a mouse model of transient cerebral ischemia. *J Cereb Blood Flow Metab* (2016). doi:10.1177/0271678X16676825
5. Klohs J, Gräfe M, Graf K, Steinbrink J, Dietrich T, Stibenz D, et al. In vivo imaging of the inflammatory receptor CD40 after cerebral ischemia using fluorescent antibody. *Stroke* (2008) 39:2845–52. doi:10.1161/STROKEAHA.107.509844
6. Morscher S, Driessen WHP, Clausen J, Burton NC. Semi-quantitative multi-spectral optoacoustic tomography (MSOT) for volumetric PK imaging of gastric emptying. *Photoacoustics* (2014) 2:103–10. doi:10.1016/j.pacs.2014.06.001
7. Kruger RA, Kiser WL, Reinecke DR, Kruger GA, Miller KD. Thermoacoustic molecular imaging of small animals. *Mol Imaging* (2003) 2:113–23. doi:10.1162/153535003322331993
8. Burton NC, Patel M, Morscher S, Driessen WH, Claussen J, Beziere N, et al. Multispectral opto-acoustic tomography (MSOT) of the brain and glioblastoma characterization. *Neuroimage* (2013) 65:522–8. doi:10.1016/j.neuroimage.2012.09.053
9. Vaas M, Ni R, Rudin M, Kipar A, Klohs J. MCAO ECA damage. *figshare* (2017). doi:10.6084/m9.figshare.4635670.v1
10. Froud MD. Studies on the arterial system of three inbred strains of mice. *J Morphol* (1959) 104:441–78. doi:10.1002/jmor.1051040304
11. Steinau H-U. *Major Limb Replantation and Postischemia Syndrome: Investigation of Acute Ischemia-Induced Myopathy and Reperfusion Injury*. New York: Springer Verlag (1988). p. 9–23, 26, 33.
12. Springer J, Schust S, Peske K, Tschirner A, Rex A, Engel O, et al. Catabolic signaling and muscle wasting after acute ischemic stroke in mice: indication for a stroke-specific sarcopenia. *Stroke* (2014) 45:3675–83. doi:10.1161/STROKEAHA.114.006258
13. Blaisdell FW. The pathophysiology of skeletal muscle ischemia and the reperfusion syndrome: a review. *Cardiovasc Surg* (2002) 10:620–30. doi:10.1016/S0967-2109(02)00070-4
14. Cafferata HT, Robinson AJ, Blaisdell FW. Coagulation changes in regional ischemia. *Surg Forum* (1968) 19:1–26.
15. Jacobsen KR, Fauerby N, Raida Z, Kalliokoski O, Hau J, Johansen FF, et al. Effects of buprenorphine and meloxicam analgesia on induced cerebral ischemia in C57BL/6 male mice. *Comp Med* (2013) 63:105–13.
16. Denes A, Pradillo JM, Drake C, Buggey H, Rothwell NJ, Allan SM. Surgical manipulation compromises leukocyte mobilization responses and inflammation after experimental cerebral ischemia in mice. *Front Neurosci* (2014) 7:271. doi:10.3389/fnins.2013.00271

Conflict of Interest Statement: The authors declare that the research was conducted in the absence of any commercial or financial relationships that could be construed as a potential conflict of interest.

Copyright © 2017 Vaas, Ni, Rudin, Kipar and Klohs. This is an open-access article distributed under the terms of the Creative Commons Attribution License (CC BY). The use, distribution or reproduction in other forums is permitted, provided the original author(s) or licensor are credited and that the original publication in this journal is cited, in accordance with accepted academic practice. No use, distribution or reproduction is permitted which does not comply with these terms.